

Influence of the precursors in the morphology, structure, vibrational order and optical gap of nanostructured ZnO

J.F. Jurado, A. Londoño-Calderón, F.F. Jurado-Lasso and, J.D. Romero-Salazar

Laboratorio de Propiedades Térmicas Dieléctricas de Compositos, Departamento de Física y Química,

Universidad Nacional de Colombia, A.A 127, Manizales, Colombia,

e-mail: jffjurado@unal.edu.co

Received 25 March 2014; accepted 23 May 2014

The synthesis of ZnO by reaction in solid state from two precursor salts (zinc acetate and zinc sulfate), presented significant differences concerning morphology, structure, vibrational order and optical gap. As well as covering in the size of the compounds, a homogeneous distribution of nanoparticles of 21 ± 3 nm and microstars of 1.03 ± 0.19 μm respectively. The ZnO showed a structural phase with a vibrational state of the hexagonal type (wurtzite). The variation in the morphology due to the precursor is attributed to the disorder within of lattice, which contributes to vibrational changes and is correlated to the degrees of freedom of molecules. Measurements of UV-Vis of nanoparticles displayed a band gap (E_g) lower than the one reported for the bulk material.

Keywords: Optical properties; nanorods; nanocrystalline; X-ray diffraction.

PACS: 78.67.Bf; 78.67.Qa; 78.67.Bf; 61.05.cp

1. Introduction

Zinc oxide is a semiconductor with band gap energy close to 3.37 eV considering its value highly promising for manufacturing and application of electronic and optoelectronic devices, such as gas nanosensors [1–3], light emitting diodes [4], solar panels [5–7], among others [8–10]. The control on its nanometric morphology is a field of great interest due to the wide range of use of low cost techniques, which allow high quality synthesis as: hydrothermal [12, 13], sol-gel [14], thermal decomposition [15, 16], solid state reaction [17, 18] among others [25]. The latter allows synthesizing polycrystalline solids from reactions which are generally in solid state. The main advantage of using this type of methodology is the non-utilization of solvents, which entails a production cost decrease. In the synthesis of ZnO nanostructures by reaction in a conventional solid state, it is thought that the greatest difficulty lies in the precise control of variables as precursor stoichiometry, maceration time and drying temperature, which are determinant parameters in the oxide morphology. Different from this conventional method, many authors have reported very successful results in nanostructures elaboration discarding high temperature thermal process [17, 19–22]. In this paper there are shown structural, vibrational, optical and morphological changes in ZnO nanostructures, obtained by reaction in solid state, from two precursors. The structural characterization of the compounds was carried out by using a X-ray Bruker D8 Advance diffractometer (radiation of $\text{CuK}\alpha$, $\lambda = 1.5406$ Å). The vibrational order was assessed throughout micro-Raman (μ -Raman Confocal LabRam HR Horiba Jobin Yvon) with a monochromatic radiation source of 473 nm. The band gap was assessed by using a UV/Vis Perkin Elmer Lambda 20 spectrophotometer. The morphology was analyzed with a Hitachi SEM-5500 Scanning electron microscope.

2. Experimental Details

For the synthesization process, were used the following compounds: As zinc salt precursors were used dehydrated zinc acetate $\text{Zn}(\text{CH}_3\text{COO})_2 \cdot 2\text{H}_2\text{O}$ and heptahydrated zinc sulfate $\text{ZnSO}_4 \cdot 7\text{H}_2\text{O}$. As an OH⁻ ion source sodium hydroxide NaOH and as a complexing agent TEA or triethanolamine $\text{N}(\text{CH}_2\text{CH}_2\text{OH})_3$. In the process, were used two powder samples of ZnO following the methodology for reaction in solid state and varying the zinc precursor salt [19]: 2.19 g (0.01 mol) of the zinc precursor salt macerated during 5 minutes, afterwards, it was added 1 ml of TEA followed by 5 minutes of maceration to obtain homogeneous material. The material obtained was a white and hard paste which is left to rest at room temperature, then it was added 0.8 g (0.02 mol) of NaOH and it was macerated during 40 minutes. The resulting material was washed repeatedly with deionized water and ultrasound assisted ethanol, in order to scatter the particles and possible residual agents that could be found in the structure. Finally, the obtained solution was left to dry in the air at a 70°C temperature

3. Results and Discussion

3.1. Morphology

Figure 1 shows SEM micrographs for the sample obtained from zinc acetate. The obtained material demonstrates a clear conformation of agglomerated nanoparticles and with a coalescence tendency. This phenomenon is principally attributed to the thermal treatment which causes the material to become compact during the drying process, also to the unstable zinc hydroxide conformation and to other compounds that were not completely removed during the washing process. The

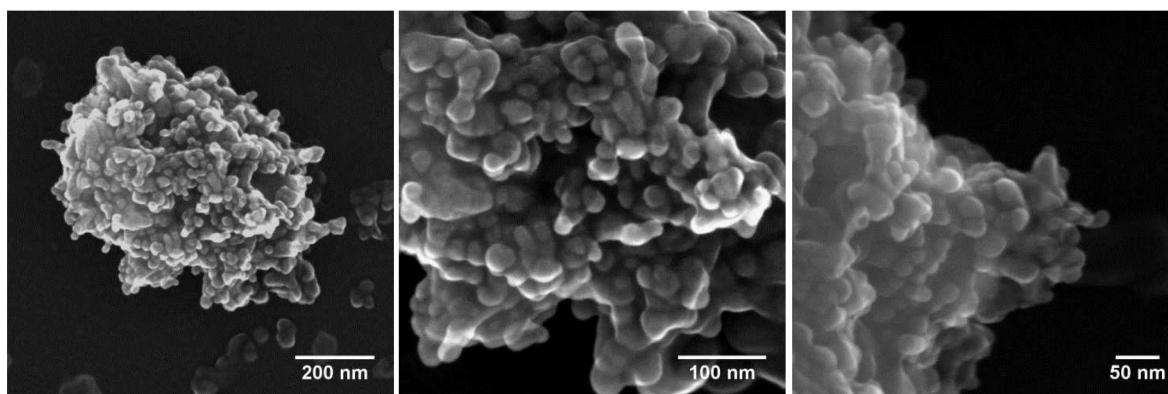


FIGURE 1. SEM images of nanoparticles ZnO powder from zinc acetate.

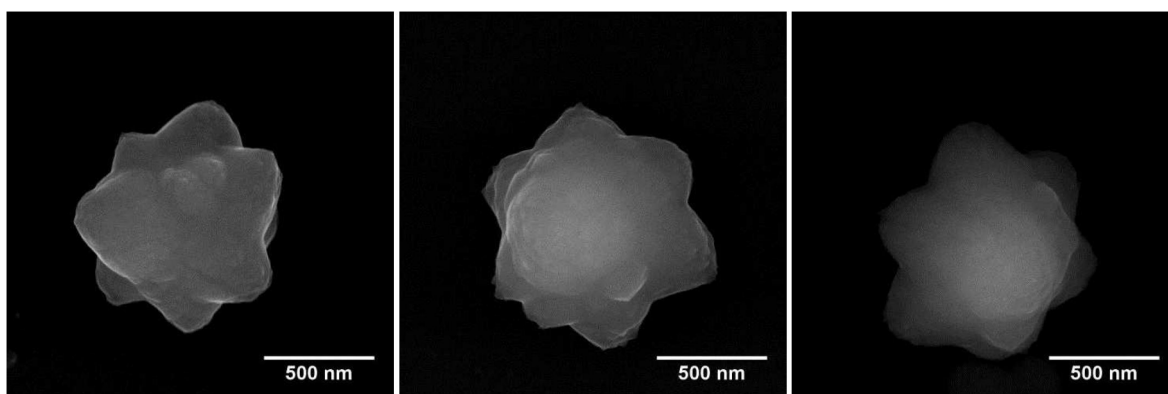


FIGURE 2. Representative SEM micrographs of ZnO micro-star synthesized from zinc sulfate.

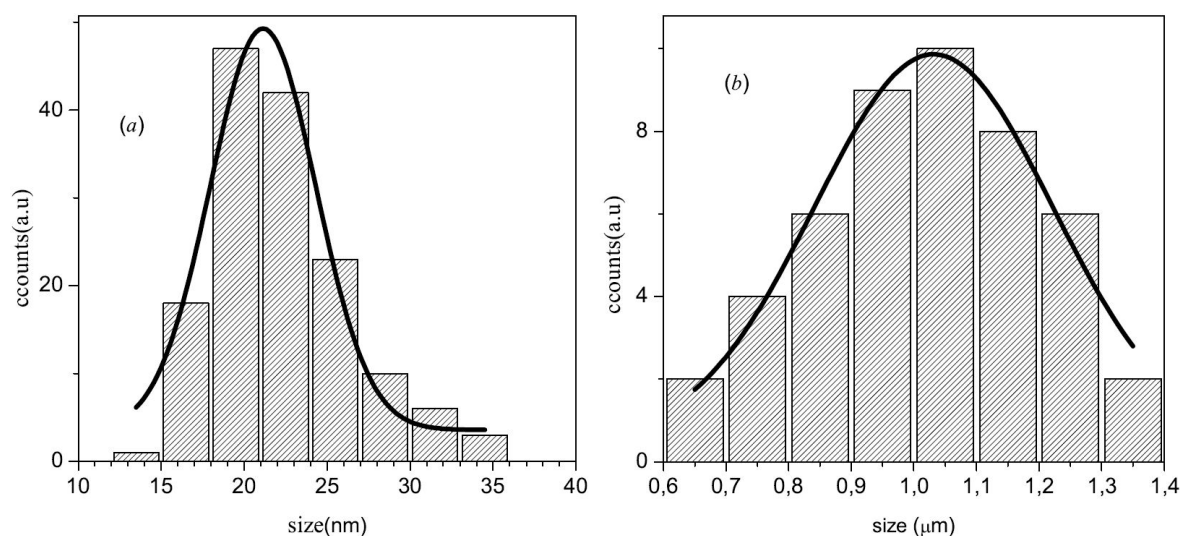


FIGURE 3. ZnO nanoparticles size distribution synthesized from, (a) zinc acetate and (b) zinc sulfate respectively.

average size of the nanoparticles was of 21 ± 3 nm. Figure 2, presents SEM micrographs for the obtained material from zinc sulfate. The morphology that can be seen is a type of microstars with an average size (among the corners) of 1.03 ± 0.19 μm . With the assistance of ImageJ Software, the size distribution histograms for the material were calculated (Fig. 3a and Fig. 3b).

3.2. Structural Properties

The crystalline order of the nanoparticles was assessed through X-ray diffraction. Figure 4 shows the diffractogram for the ZnO obtained from the two precursors and JCPDS card no. 01-080-0075 respectively. Both compounds present a structure which corresponds to the hexagonal phase

TABLE I. Lattices parameters and crystallite size.

Starting reactive	a (Å)	c (Å)	D (Å)
Zinc acetate	3.2538 ± 0.0003	5.2086 ± 0.0013	143 ± 8
Zinc sulfate	3.2516 ± 0.0001	5.2082 ± 0.0004	191 ± 9

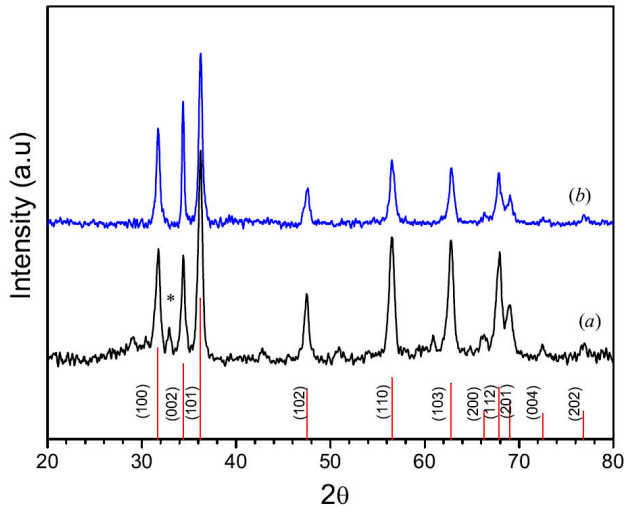


FIGURE 4. X-Ray diffraction patterns of ZnO nanoparticles synthesized from: a) zinc acetate and b) zinc sulfate. The solid lines are the intensities and diffraction indexes according JCPDS no. 01-080-0075. * is due to hidroncincita phase.

(wurtzite) of zinc oxide. Table I shows the structural parameters a and c calculated from Cohen method. The crystallite size (D) was established from Scherrer equation. These parameters are compared to the reported values for the ZnO according to JCPDS card no.01-080-0075. For the obtained material form zinc acetate, the diffraction presents an additional phase (marked *) located approximately in $2\theta=32.9^\circ$ which is associated with the conformation of zinc complex $Zn_5(CO_3)_2(OH)_6$ hydrozincite, which indicates ion excess of Zn^{2+} in the material during the reaction. The value of lattice parameters a and c are not significantly far from the value reported for the bulk material. Crystallite size for the material

is the same type as nanoparticles size, which demonstrates that every particle is conformed by 1 and 2 crystallites. For the material obtained from zinc sulfate, the diffraction does not present additional phases. The values for lattice parameters are lower than the values reported in the literature. Microstars are highly polycrystalline when conformed by many crystallites.

3.3. Vibrational Properties

Figure 5 shows Raman spectra of the synthesized material in this work and powder ZnO. There are presented six normal vibrational modes which correspond to the literature reports for ZnO [23]. In Table II are listed the modes and location, as well as the intensity relationship (I_i/I_0), being I_0 the intensity for the most intense mode called $E_2(\text{high})$. Longitudinal optical modes $A_1(\text{LO})$ y $E_1(\text{LO})$ are not in the reference material, due to the fact that they are only visible when the axis c of wurtzite structure is parallel to the surface. In the case of nanostructured material there are no constraints for longitudinal optical modes since the structures are randomly positioned [22]. For the synthesized sample from zinc acetate, it is shown a reduction in the mode intensity which are related to the configuration of oxygen atoms $A_1(\text{TO})$ and $A_1(\text{LO})$ of flexion symmetrical movements. This statement suggests a stoichiometric loss of oxygen atoms. The mode $E_1(\text{LO})$ which is related to oxygen defect or vacancy is not found [24]. This absence demonstrates that during oxygen loss the structure reorganizes conforming zinc complexes such as hydrozincite, as observed during the X-ray diffraction pattern. Multiphonic mode intensity $E_{2H} - E_{2L}$ y $E_{2H} + E_{2L}$ are highly dependable on the disorder degree in the lattice, which entails a relation with the material morphology. For ZnO microstars synthesized from zinc sulfate, the variations in the vibrational order within bulk material are not relevant, except from the multiphonic mode increase $E_{2H} + E_{2L}$ and the presence of the optical longitudinal mode A_1 which is correlated to the disorder degree of the material. It is not demonstrated the presence of the mode $E_1(\text{LO})$ which is related to oxygen defects and vacancies in the material.

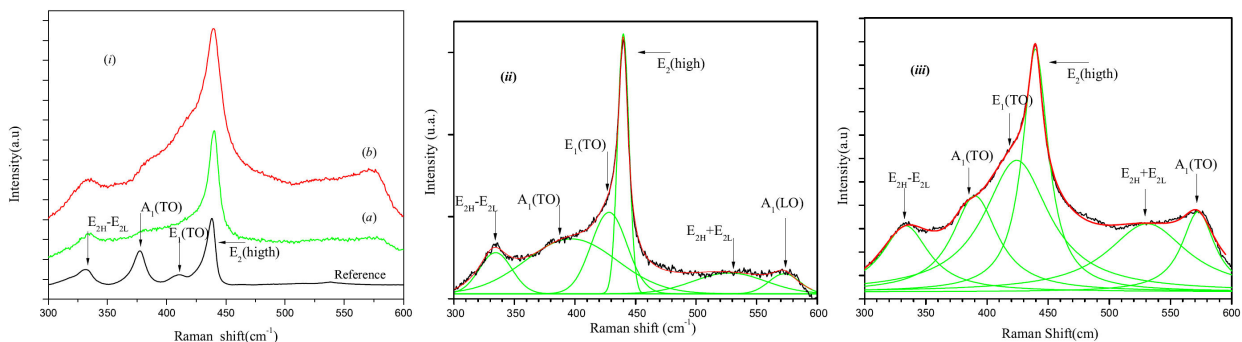


FIGURE 5. Micro-Raman spectra of ZnO nanostructured synthesized from; i)(a) zinc acetate, (b) zinc sulfate and powder (reference), (ii) and (iii) Adjustments to the location of the vibrational modes obtained from acetate and zinc sulfate.

TABLE II. ZnO vibrational mode and relative intensity

Mode	Reference		Zinc Acetate		Zinc Sulfate	
	Wavelength (cm ⁻¹)	I_i/I_0	Wavelength (cm ⁻¹)	I_i/I_0	Wavelength (cm ⁻¹)	I_i/I_0
$E_{2H}-E_{2L}$	328	26.5	332	17.6	333	39.9
$A_1(\text{TO})$	376	57.8	392	27.7	390	49.3
$E_1(\text{TO})$	410	19.4	428	21.1	424	61.5
$E_2(\text{high})$	437	100	440	100	440	100
$E_{2H}+E_{2L}$	536	4.5	527	14.3	531	40.6
$A_1(\text{LO})$	-	-	573	7.7	573	44.3
$E_1(\text{LO})$	-	-	-	-	583	4.7

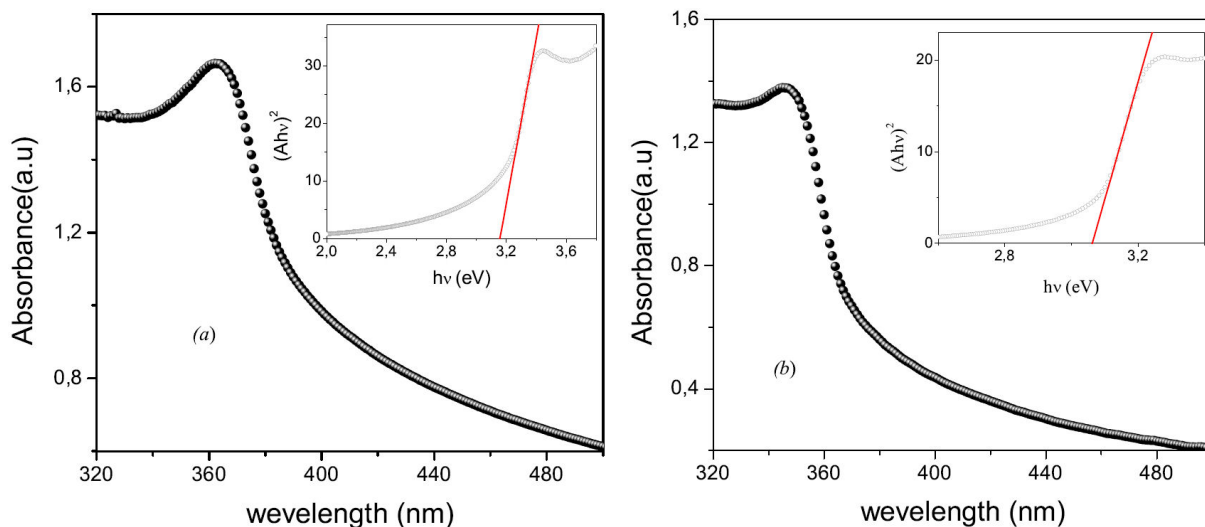


FIGURE 6. Absorbance of ZnO nanostructured synthesized from; (a) zinc acetate and (b) zinc sulfate. The inset shows the extrapolation to determine E_g . The solids lines are the best fit.

3.4. Optical Absorption

Figure 6 shows the absorption of the synthesized material from zinc acetate and zinc sulfate. From this measurements, it can be established the energy of the band gap (E_g) by utilizing the Tauc equation

$$Ah\nu = B(h\nu - E_g)^m \tag{1}$$

Where A is the absorption, B is a constant and constant m is taken as $1/2$, for direct transition materials. From graph $(Ah\nu)^2$ based on the energy (inset Fig. 6), axis division corresponds to the energy E_g , which results in: 3.16 ± 0.03 y 3.06 ± 0.06 eV for zinc acetate and sulfate, showing a decrease in comparison to the bulk material of 3.37 eV.

4. Conclusions

Throughout the synthesizing of ion reaction in solid state, it was accomplished to obtain ZnO nanoparticles and microstars from dehydrated zinc acetate and heptahydrated zinc

sulfate. The material obtained from zinc acetate showed a mixture of the hexagonal phase (wurtzite) and hydrozincite, being this last phase related to an ion excess Zn^{2+} . The material presented a decrease in the vibrational modes related to oxygen sub-lattice. The material obtained from zinc sulfate showed a hexagonal phase (wurtzite) with smaller lattice parameters in comparison to the bulk material parameters, which is related to constraints imposed by the morphology type. ZnO microstars showed an increase in the multiphonic mode $E_{2H} + E_{2L}$ and the appearance of longitudinal optical mode A_1 which entails a greater disorder degree. The non presence of the mode $E_1(\text{LO})$ is related to the increase of oxygen defect and vacancies in the material.

Acknowledgments

This work was supported by the Research Direction of Manizales DIMA from National University of Colombia-Project number 15875. The authors wish to thank to: Plasma physics, Material optical properties and Chemistry laboratories for the

XRD, Raman and UV-Vis measurements. As well as the University of Texas, at Antonio and Kleberg Advanced Microscopy Laboratory where the SEM measurements were carried out.

1. O. Lupan *et al.*, *Materials Research Bulletin* **45** (2010) 1026.
2. K. Kim, H. R. Kim, K. I. Choi, H. J. Kim, and J. H. Lee, *Sensors and Actuators B* **155** (2011) 745.
3. M. M. Arafat, B. Dinan, S. A. Akbar, and A. S. M. A. Haseeb, *Sensors* **12** (2012) 7207.
4. P. C. Tao, Q. Feng, J. Jiang, H. Zhao, R. Xu, S. Liu, M. Li, J. Sun, and Z. Song, *Chemical Physics Letters* **522** (2012) 92.
5. C. Luan *et al.*, *Nanoscale Research Letters* **6** (2011) 340.
6. N. Singh, R. M. Mehra, A. Kapoor, and T. Soga, *Journal of renewable and sustainable energy* **4** (2012) 013110.
7. M. Navaneethan, J. Archana, M. Arivanandhan, and Y. Hayakawa, *Chemical Engineering Journal* **213** (2012) 70.
8. G. C. Yi, T. Yatsui, and M. Ohtsu, *Comprehensive Nanoscience and Technology: Nanomaterials* **1** (2011) 335.
9. C. Ma, Z. Zhou, H. Wei, Z. Yang, Z. Wang, and Y. Zhang, *Nanoscale Research Letters* **6** (2011) 536.
10. Y. Zhang, M. K. Ram, E. K. Stefanakos, and D. Y. Goswami, *Journal of Nanomaterials* **2012** (2012) 1.
11. L. Schmidt- mende and J. L. Macmanus- driscoll, *Materials today* **10** (2007) 40.
12. H. Xu, H. Wang, Y. Zhang, W. He, M. Zhu, B. Wang, and H. Yan, *Ceramics International* **30** (2004) 93.
13. H. Wang, J.Xie, K. Yan, M.Duan, *Journal of Materials Sciences and Technology* **27** (2011) 153.
14. B. Karthikeyan and T.Pandiyarajan, *Journal of Luminescence* **130** (2010) 2317.
15. C.Wua, L.Shen, Q. Huang, and Y. C. Zhang, *Powder Technology* **205** (2011) 137.
16. C.Wun and Q. Huang, *Journal of Luminescence* **130** (2010) 2136.
17. Y. Cao, P. Hu, W. Pan, Y. Huang, and D.Jia, *Sensors and Actuators B* **134** (2008) 462.
18. C. F. Jin, X. Yuan, W. W.Ge, J. M. Hong, and X. Q.Xin, *Nanotechnology* **14** (2003) 667.
19. X. Jia, H. Fan, M.Afzaal, X. Wu, and P. O'Brien, *Journal of Hazardous Materials* **193** (2011) 194.
20. A. Sugunan, H. C.Warad, M.Boman, and J.Dutta, *Journal of Sol-Gel Science and Technology* **39** (2006) 49.
21. A. Jana, N. R.Bandyopadhyaya, and P. S. Devi, *Solid State Sciences* **13** (2011) 1633.
22. R. Zhang, P. G. Yin, N. Wang, and L.Guo, *Solid State Sciences* **11** (2009) 865.
23. W.Guo, T. Liu, L. Huang, H. Zhang, Q. Zhou, and W.Zeng, *Physica E* **44** (2011) 680.
24. M. S. Soosen, K. Jiji, C. Anoop, and K. C. George, *Indian Journal of Pure and Applied Physics* **48** (2010) 703.
25. M. Navaneethan, J. Archana and Y. Hayakawa, *Chemical Engineering Journal*, **15** (2013) 8246.